S- and X-Band RF Feed System

P. D. Potter
Communications Elements Research Section

To support the Mariner 1973 X-band experiment, it will be necessary to implement a dual-frequency microwave feed system for the DSS 14 64-m antenna. This system must be capable of simultaneous low noise reception at S- and X-bands and high power transmission at S-band. To fulfill this requirement, a particularly attractive approach, the reflex feed system, is being implemented. The system makes simultaneous use of both an X-band feedcone and one of the S-band feedcones. By a system of two reflectors, one of which is dichroic, the effective S-band phase center is translated from its normal position in the S-band feedhorn to a new point which very nearly coincides with the X-band feedhorn phase center. Thus, during simultaneous S- and X-band operation, the antenna subreflector optics are aligned with the X-band feedcone position. This article describes the analytical techniques used to design and analyze the feed system, as well as preliminary results from scale model tests.

I. Introduction

A cross-sectional view of the reflex feed system[1] geometry is shown to scale in Fig. 1. The system is comprised of four basic components: the S-band feedhorn centrally located in its feedcone, an ellipsoidal reflector, a planar dichroic reflector, and the X-band feedhorn centrally located in its feedcone. By reciprocity, the operation of the reflex feed is the same in the receiving mode as in the transmitting mode; for simplicity, Fig. 1 shows only the transmitting mode. For S-band operation, from a geometrical optics standpoint, radiated energy from one of the ellipsoid foci f_1 is focused to the point f_2. As shown in Fig. 1, however, the system is not large compared to a wavelength. Because of this consideration and the fact that the S-band feedhorn does not represent a point source, the radiated energy from the ellipsoid is actually found to focus to a small region centered at the point C. This energy is then redirected by the planar reflector to the antenna subreflector. By the principle of images, this redirected radiation appears to emanate from the point F_X, which is the far-field phase center of the X-band feedhorn and also coincides with one of the subreflector foci. To permit simultaneous X-band operation, the central region of the planar reflector is perforated with an array of X-band slots, thereby making the reflector essentially transparent to X-band but reflective to S-band.

A preliminary design for the dichroic plate has been extensively tested and previously described (Ref. 2). Although this design has acceptable performance, a continuing effort is in progress to study the S- and X-band performance as a function of the plate thickness and the detailed slot design.

[1]A brief description of the reflex feed system is given in Ref. 1.

II. Analytical Techniques Used for Design and Analysis

An existing scattering program (Ref. 3) was modified[2] to accept general quadratic scattering surfaces and was utilized to calculate the far-field radiation patterns of the S-band horn and ellipsoidal reflector combination. This program was thus used to study and optimize the ellipsoid geometry in order to produce a scattered radiation pattern very similar to the radiation pattern of the horn by itself. The horn pattern has been previously optimized for correct subreflector illumination. The phase of the ellipsoid scattered fields was used to locate the point C (Fig. 1) for a practical overall geometry.

Unlike present and past DSS 14 feed systems, the reflex feed does not have physical rotational symmetry about the axis of symmetry of the antenna subreflector. For this reason, the reflex feed radiation pattern does not exhibit the high level of pattern symmetry which the horns have. To investigate the magnitude of the resulting antenna gain degradation due to this effect, spherical wave techniques were utilized. In the spherical wave method, a radiation pattern is expanded in a series of orthogonal waves which have a known mathematical dependence on the polar angle θ, the azimuthal angle ϕ and the radius R. The details of spherical wave analysis are well documented in the literature (Refs. 3, 4, and 5) and will not be repeated here.

The azimuthal dependence of the feed radiation is represented as a Fourier series as follows:

$$E_\theta(\theta,\phi,R) = \sum_{m=1}^{M} E_{\theta me}(\theta,R)\sin(m\phi) \quad \text{(EVEN)} + \sum_{m=0}^{M} E_{\theta mo}(\theta,R)\cos(m\phi) \quad \text{(ODD)} \tag{1}$$

$$E_\phi(\theta,\phi,R) = \sum_{m=0}^{M} E_{\phi me}(\theta,R)\cos(m\phi) \quad \text{(EVEN)} + \sum_{m=1}^{M} E_{\phi mo}(\theta,R)\sin(m\phi) \quad \text{(ODD)} \tag{2}$$

In Eqs. (1) and (2), $E_\theta(\theta,\phi,R)$ and $E_\phi(\theta,\phi,R)$ are given radiation patterns to be represented as a truncated Fourier series. It is easily shown (Ref. 6) that only the $m = 1$ components of the pattern contribute to the antenna gain. Energy contained in $m \neq 1$ components represents a degradation of antenna gain and, also, in the receive mode, a possible source of system noise temperature degradation. Figure 2 shows the form of the component radiation patterns for the first four m dependences.

A new computer program was developed to compute the azimuthal component patterns as given by Eqs. (1) and (2). The input to this program is a group of radiation patterns which may be either experimental or obtained from the previously described scattering program. The program output is a series of polar patterns for each m index up to M, together with the total powers in each of the m-component patterns. This program was first utilized to analyze the ellipsoid scattered fields. The resulting modal power distribution is shown in Fig. 3. As would be expected from the geometry shown in Fig. 1 and the patterns shown in Fig. 2, the dominant extraneous energy is in the $m = 0$ and $m = 2$ modes. The gain degradation factor of 0.10 dB from pattern asymmetry is considered acceptable.

To calculate the scattered fields from the flat plate, the $m = 0$ and 2 patterns were first expanded in spherical polar modes (Ref. 3) about the point C. The resulting mode coefficients were then utilized in the scattering program (Ref. 3) to calculate the scattered fields from the flat plate.

III. Comparison of Computed and Measured Data

Since the reflex feed design is based on a series of computer programs which are novel in some respects, it was necessary to experimentally validate the design by scale model testing. Three 1/7-scale model ellipsoid designs have been tested in the JPL Mesa Antenna Range anechoic chamber. The three designs differed in the beamwidth of scattered fields: the first two bracketing, and the final being essentially the same as the standard feedhorn. Figures 4 and 5 show the excellent agreement between the computed and measured elipsoid patterns, thus validating the scattering program design. For these patterns the feedhorn was polarized perpendicular to the plane of Fig. 1. Patterns taken with the orthogonal polarization were essentially identical.

Scale model patterns were also taken of the complete feed including the flat plate (planar reflector); these are compared with the computed patterns in Figs. 6 and 7. The computational technique was that described in *Section II*, above, using the $m = 0$, 1, and 2 pattern components. A comparison of these two figures with Figs. 4 and 5 shows that, even though the planar reflector is relatively small, it behaves very nearly as predicted by image

[2]Private communication from R. A. Norman, JPL Communications Elements Research Section.

theory. By resolution of the flat plate scattered patterns into m-component patterns, it was also determined that reflection from the flat plate does not significantly change the energy distribution between the m modes, i.e., orthogonality is maintained.

IV. Present Efforts

Several efforts are presently being pursued by the Communications Elements Research Section. Reduction and analysis of scale model data for the third and final ellipsoid design is in progress. Additional scale model tests are being undertaken in which the relative geometry of the four reflex feed component parts is perturbed and the effect on system performance is evaluated. Both experimental and analytical data on the power dissipation/temperature profile of the ellipsoid and flat plate under high power S-band transmission are being developed. Further tests and calculations of the dichroic plate design are being undertaken for optimization of the slot configuration.

References

1. Katow, M., "S- and X-Band RF Feed System," in *The Deep Space Network Progress Report*, Technical Report 32-1526, Vol. VI, pp. 139–141. Jet Propulsion Laboratory, Pasadena, Calif., Dec. 15, 1971.
2. Woo, R., "A Low-Loss Circularly Polarized Dichroic Plate," in *1971 G-AP International Symposium Digest*, pp. 149–152, Sept. 22-24, 1971.
3. Ludwig, A. C., *Calculation of Scattered Patterns From Asymmetrical Reflectors*, Technical Report 32-1430. Jet Propulsion Laboratory, Pasadena, Calif., Feb. 15, 1970.
4. Potter, P. D., "Application of Spherical Wave Theory to Cassegrainian-Fed Paraboloids," *IEEE Trans. Ant. Prop.*, Vol. AP-15, No. 6, pp 727–736, Nov. 1967.
5. Ludwig, A. C., "Near-Field Far-Field Transformations Using Spherical-Wave Expansions," *IEEE Trans. Ant. Prop.*, Vol. AP-19, No. 2, pp. 214–220, Mar. 1971.
6. Rusch, W. V. T., and Potter, P. D., *Analysis of Reflector Antennas*, pp. 78–81. Academic Press, New York, 1970.

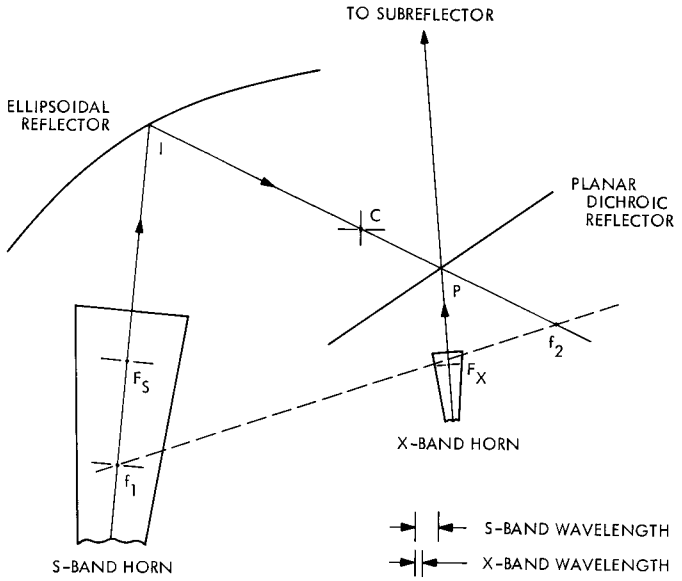

Fig. 1. Reflex feed system

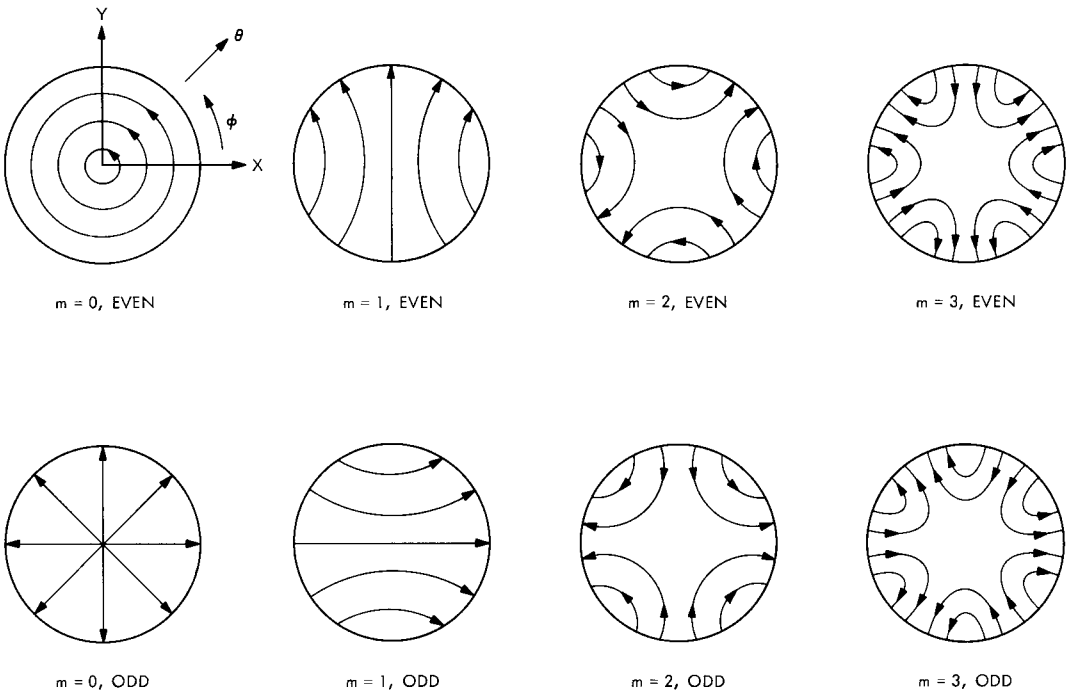

Fig. 2. Physical interpretation of *m* dependence

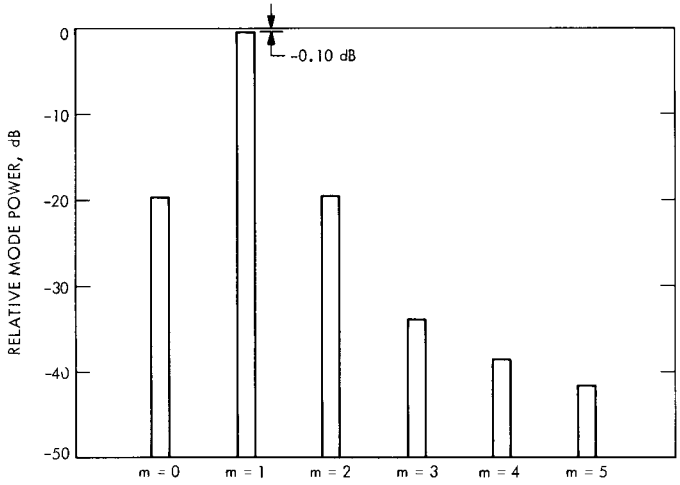

Fig. 3. Ellipsoid pattern azimuthal mode power

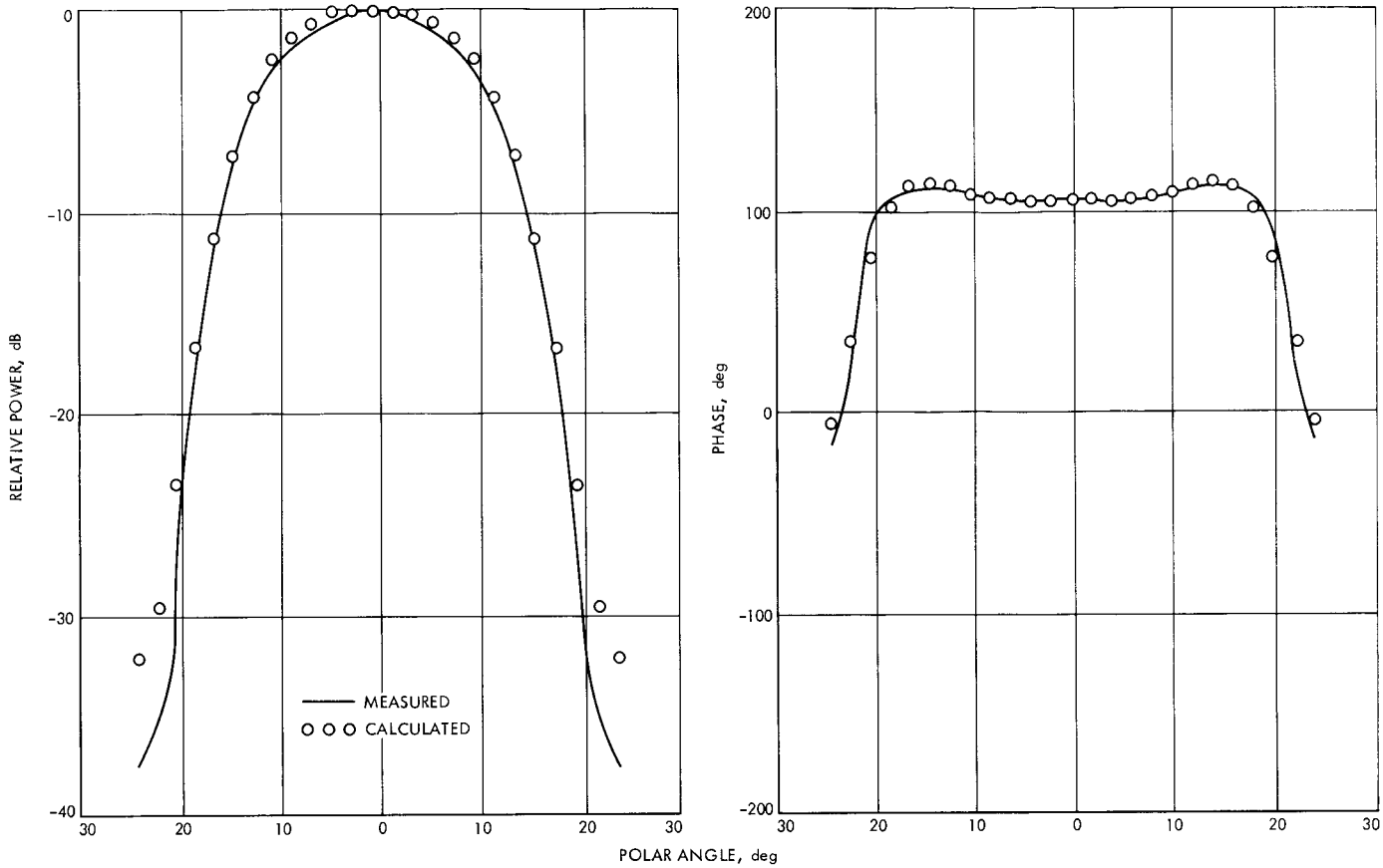

Fig. 4. E-plane ellipsoid patterns, design 1

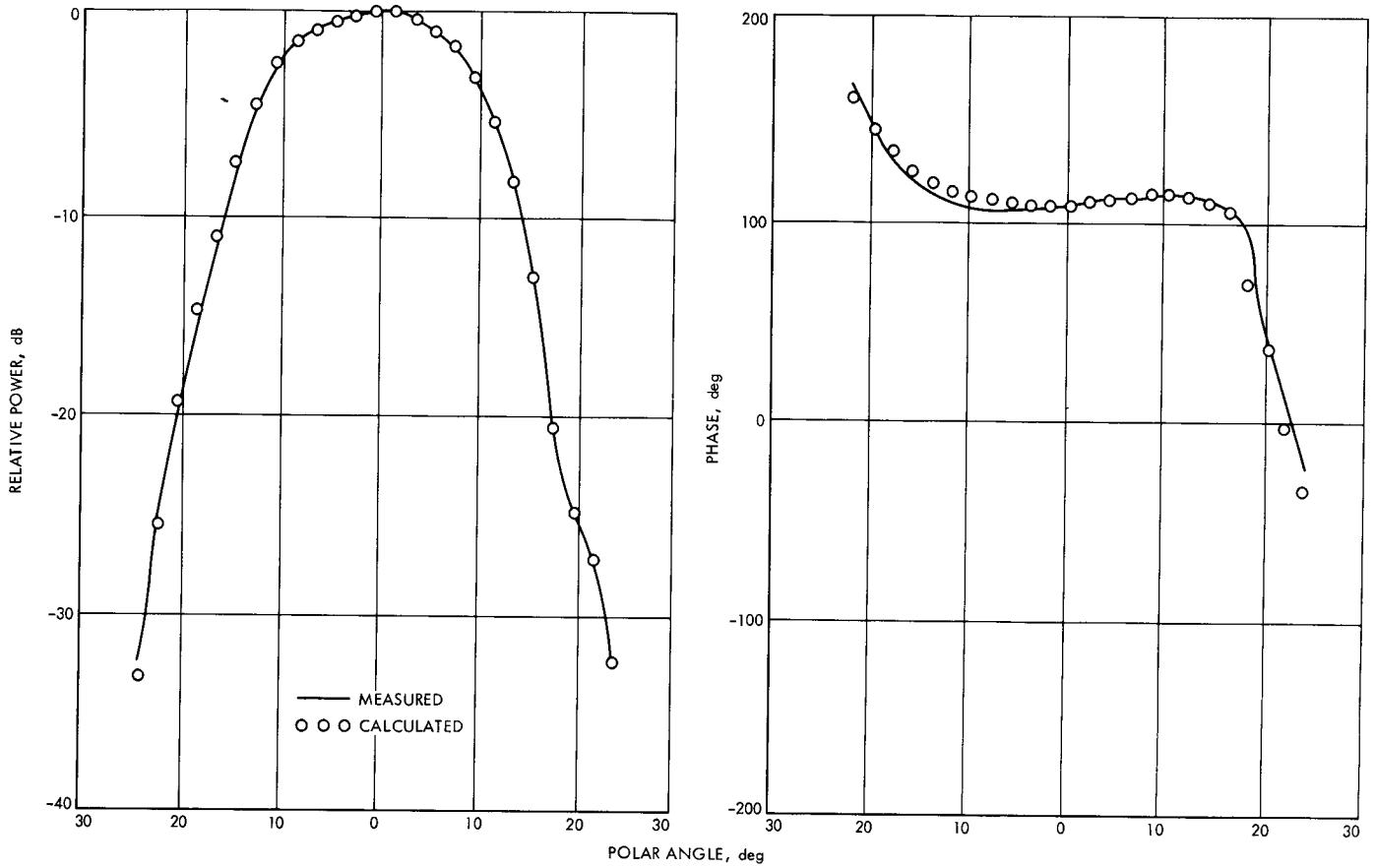

Fig. 5. H-plane ellipsoid patterns, design 1

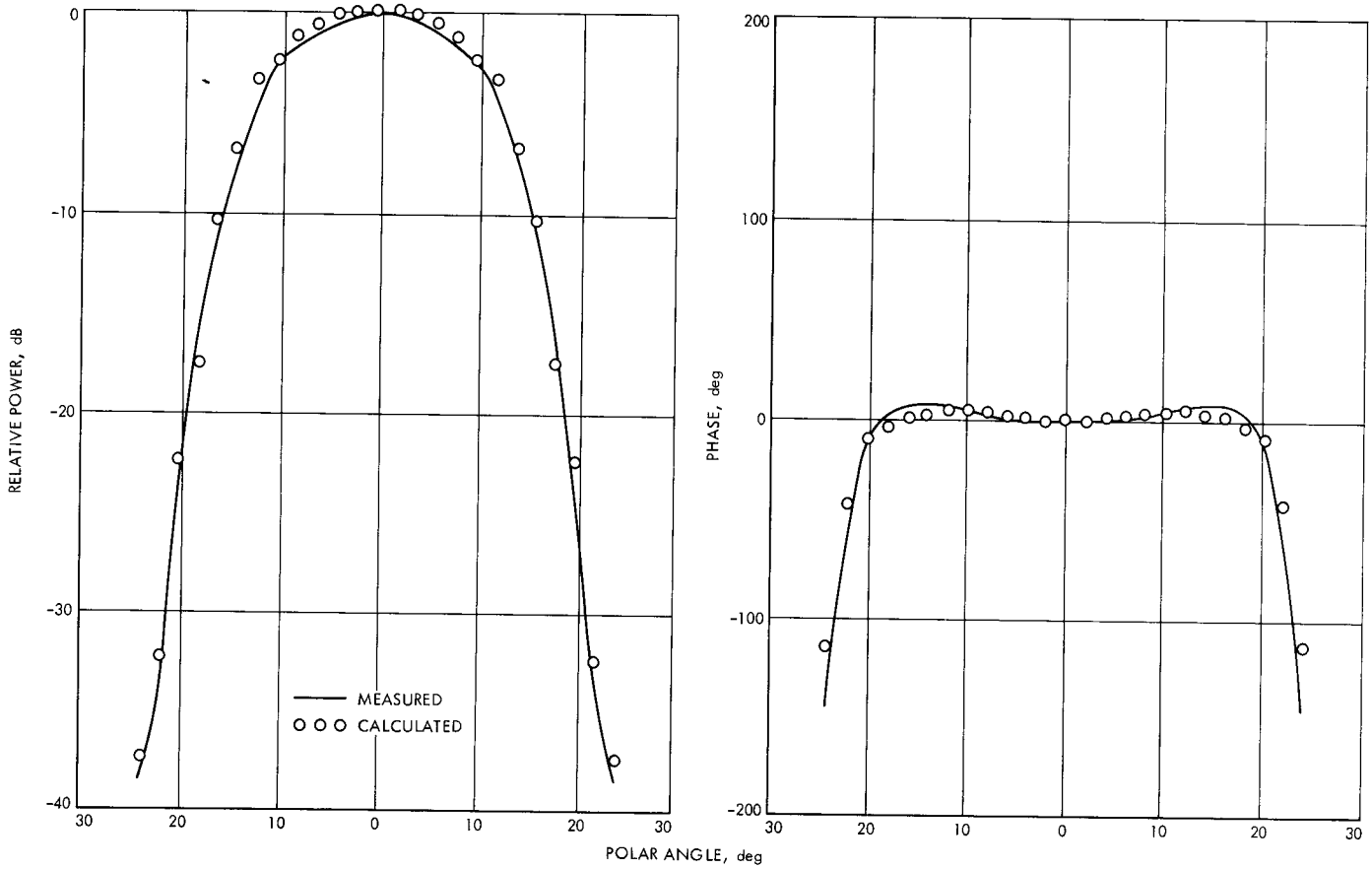

Fig. 6. E-plane flat plate patterns, design 1

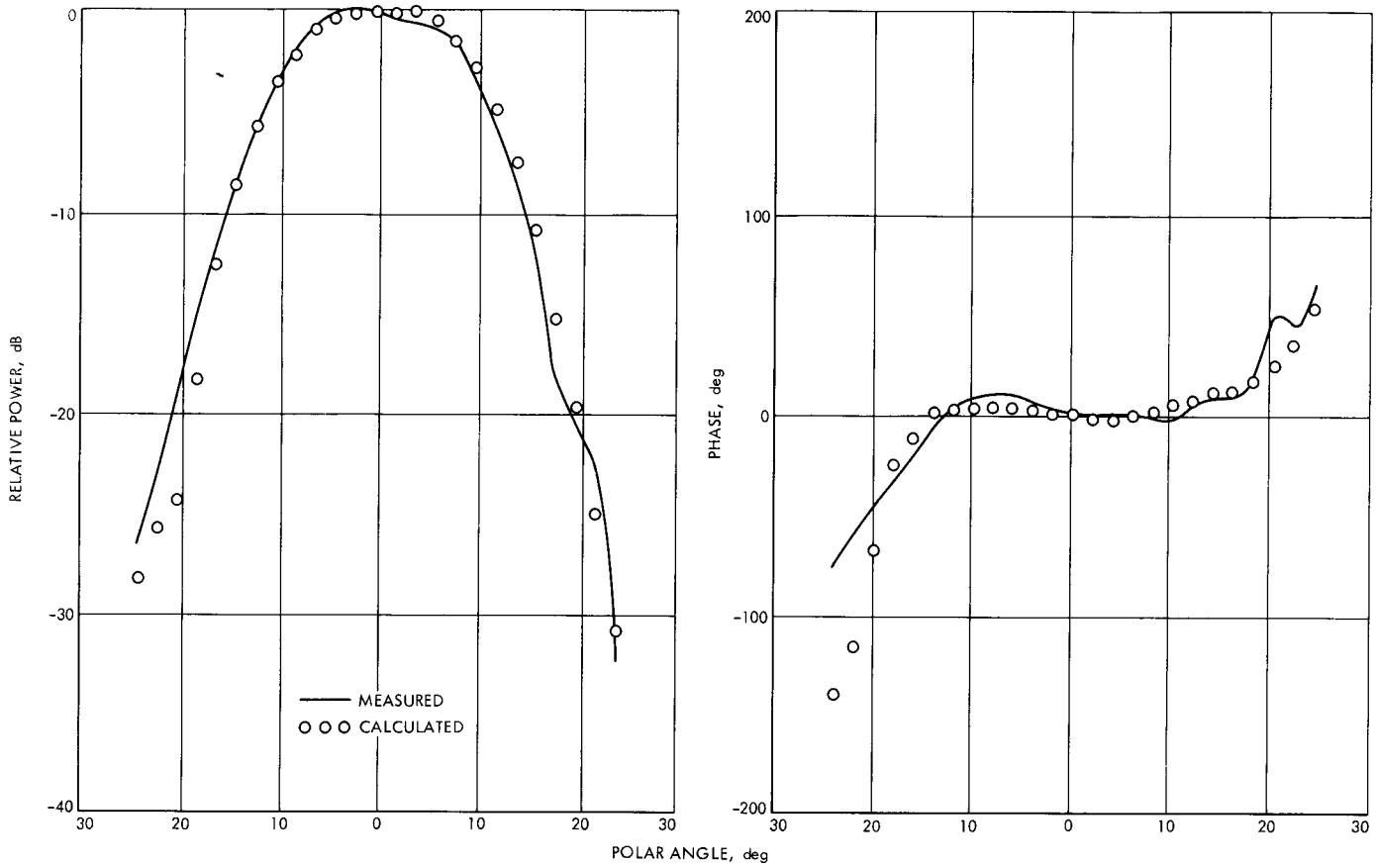

Fig. 7. H-plane flat plate patterns, design 1